

Research article

Field scale nitrogen load in surface runoff: Impacts of management practices and changing climate



Congyu Hou^a, Maria L. Chu^{a,*}, Jorge A. Guzman^a, Juan S. Acero Triana^a, Daniel N. Moriasi^b, Jean L. Steiner^b

^a Department of Ag and Bio Eng, University of Illinois, 1304 West Pennsylvania Avenue, Urbana, IL, 61801, USA

^b USDA-ARS Grazinglands Research Laboratory, 7207 West Cheyenne Street, El Reno, OK, 73036, USA

ARTICLE INFO

Keywords:

PRZM model
N load
Crop rotation
Future climate projections
Fertilizer application rate
Land management practices

ABSTRACT

The use of Nitrogen (N) fertilizer boosted crop production to accommodate 7 billion people on Earth in the 20th century but with the consequence of exacerbating N losses from agricultural landscapes. Land management practices that can prevent high N load are constantly being sought for mitigation and conservation purposes. This study was aimed at evaluating the impacts of different land management practices under projected climate scenarios on surface runoff linked N load at the field scale level. A framework to analyze changes in N load at a high spatiotemporal resolution under high greenhouse emission climate projections was developed using the Pesticide Root Zone Model (PRZM) for the Willow Creek Watershed in the Fort Cobb Experimental Watershed in Oklahoma. Specifically, 12 combinations of land management and climate scenarios were evaluated based on their N load via surface runoff from 2020 to 2070. Results showed that crop rotation practices lowered both the N load and the probability of high N load events. Spring application reduced the negative effects in summer and fall from other land management practices but at the risk of increased probability of generating high N load in April and May. The fertilizer application rate was found to be the most critical factor that affected the amount and the probability of high N load events. By adopting a target application management approach, the monthly maximum N can be decreased by 13% while the annual mean N load by 6%. The model framework and analysis method developed in this research can be used to analyze tradeoffs between environmental welfare and economic benefits of N fertilizer at the field scale level.

1. Introduction

The Haber-Bosch process developed in the 20th century brought production of Nitrogen (N) fertilizer to industrial scales, boosting crop production but with the consequence of exacerbating N losses from agricultural landscapes. In fact, studies reported that the N fertilizer loss via surface runoff and leaching processes can account for up to 1/3 and 3/4 of the total N applied (Douglas Jr. et al., 1998) and can further increase during unusual rainfall events following fertilizer application. N losses decrease N fertilizer application efficiency (Turner, 2004) prompting increase in application rates to maintain crop productivity, which will consequently, increase the N load in our water bodies. High N load can also stem from a combination of numerous causes. Researchers found that higher fertilizer application amount, shallow application depth, and fewer application times would largely increase N load from cultivated landscapes (Douglas Jr. et al., 1998; Timmons

et al., 1973). Topography is a significant factor that can lead to serious N load. Farmlands with slopes greater than 15° are not suitable for agricultural activities due to high erosion rate and N load during rainfall events (Chen et al., 2003). Land management practices that can prevent high N load are constantly being sought for mitigation and conservation purposes. For instance, researchers found that the total N load in rivers could be reduced by decreasing the N application in the area near watershed outlets (Schilling and Wolter, 2009).

Quantifying the impacts of different agricultural activities on N load requires continuous monitoring of surface runoff and N concentration over a long period to determine the spatio-temporal responses of the system to these activities. In addition, to acquire a high spatial resolution dataset, numerous monitoring stations are needed to capture the variability of the different physio-chemical processes in the system. Nonetheless, assessing the impacts of these activities is challenging due to the difficulty of identifying the factors or combination of factors that

* Corresponding author. 1304 West Pennsylvania Avenue, Urbana, IL, 61801, USA.

E-mail addresses: hou24@illinois.edu (C. Hou), mlchu@illinois.edu (M.L. Chu), jag@illinois.edu (J.A. Guzman), jsa2@illinois.edu (J.S. Acero Triana), daniel.moriasi@ars.usda.gov (D.N. Moriasi), jean.steiner@ars.usda.gov (J.L. Steiner).

<https://doi.org/10.1016/j.jenvman.2019.109327>

Received 11 March 2019; Received in revised form 22 July 2019; Accepted 28 July 2019

0301-4797/ © 2019 Elsevier Ltd. All rights reserved.

result in high N load. The N that ends up in our water bodies is driven by a combination of different agricultural activities and soil properties under the influence of the prevailing weather. Due to the challenges in carrying out long-term field experiments to predict the impacts of prevalent agricultural activities and the variability of weather systems on N load, numerical models have been widely implemented. In particular, models quantifying the impacts of different land management practices on N load have been numerous in the last decades (Wang et al., 2018). For instance, the Soil Water Assessment Tool (SWAT) is a widely used model in evaluating the impacts of different land management practices on nutrients and sediments (Wang et al., 2018). Like SWAT, the Agricultural Policy Environmental Extender (APEX) model also determines changes in water quality and quantity due to different agricultural activities that span from cropping to animal grazing (Tuppad et al., 2010; Williams et al., 2015). Similarly, the Model for N and Carbon (MONICA) predicts changes in N load from different land management practice and climate variations (Nendel et al., 2011).

Although these models are able to generally predict the impacts of agricultural activities on N , some limitations hinder their effectiveness in assessing field scale spatio-temporal variation in N . SWAT and APEX, for example, both perform simulations on sub-basin or watershed levels (Schilling and Wolter, 2009; Tuppad et al., 2010). Since land management practices are typically implemented at the local scale, the ability of these numerical models to assess changes in N at this scale is crucial. Furthermore, most model applications mainly focus on the growing seasons under average rainfall events without considering the uncertainties brought about by future climate (Schilling and Wolter, 2009). Since rainfall is the main driver of surface runoff that facilitates N losses to water bodies, assessing N load during rainfall events in a probabilistic manner is necessary.

The main objective of this study was to evaluate the impacts of the different land management practices and climate on surface runoff linked N load at the field scale level. We developed a framework to analyze changes in N load in surface runoff at a high spatio-temporal resolution under high greenhouse emission climate projections. Specifically, we determined the combination of factors that can lead to a long-term high N load under different crop rotation schemes, different fertilizer application schemes, and projected climate scenarios. To accomplish these objectives, a high spatio-temporal modeling framework using the integrated Pesticide Root Zone Model version 3 (PRZM) (Suárez, 2005) was developed for the Willow Creek Watershed in central western Oklahoma to simulate changes in N load in surface runoff. By being able to identify the factors that lead to high N load losses at a field scale level under different climate projections, focused conservation and mitigation practices can be implemented to minimize the environmental impacts of agricultural activities.

2. Materials and methods

2.1. Study area

The Willow Creek Watershed (WCW), with an area of 85.2 km², is one of the sub-watersheds of the Fort Cobb Experimental Watershed (FCREW) (Fig. 1b), which is part of the Central Great Plains Ecoregion located in central western Oklahoma (Fig. 1a). With a yearly average temperature of 16 °C and an annual precipitation of 889 mm, the WCW has a growing season of over 200 days (University of Oklahoma, 2017). The warm and mild climate in WCW allows the growing of a variety of crops as well as pasture. Based on the U.S. Department of Agriculture (USDA) National Agricultural Statistics (NASS) (USDA, 2019) Cropland Data Layer from Natural Resources Conservation Service (NRCS), about 90 percent of the area in the watershed was used for agriculture from 2006 to 2015 (NRCS, 2017). The main agricultural crops in WCW that require fertilizer were Winter Wheat (31%), Cotton (5%) and other crops that include small percentages of Sorghum and Peanuts, while Pasture (38%) is used for animal grazing. As a result, N load from

agricultural lands has become the main source of nonpoint source pollution in WCW. In addition, large amounts of cultivated land in this watershed has introduced other environmental problems including impaired water by fecal bacteria from animal grazing and excessive sediment load (Jamieson et al., 2003; Williams, 1975).

2.2. The Pesticide Root Zone Model

The PRZM was used to simulate the fate and transport of N in the WCW. PRZM is a one-dimensional, dynamic, compartmental model for use in simulating chemical movement, transformation, and fate in the unsaturated soil systems within and immediately below the plant root zone (Suárez, 2005). The inputs of the PRZM included soil properties, land use, land management practices, and climate data while streamflow and N load were used to verify the performance of the model in simulating N fate and transport (Fig. 1c). The outputs of the PRZM that were of interest in this study included surface runoff (cm day⁻¹) and N load in surface runoff (g day⁻¹ m⁻²).

2.3. Spatial discretization and model parameterization

Spatial discretization. The baseline model for the WCW was constructed from a structured grid with a 120 × 120 m cell size in which lumped responses at each cell was estimated by a PRZM model for a total of 5,911 PRZM models. The time of concentration in WCW was estimated using the Soil Conservation Service (SCS) method to be 12.5 h (USDA, 2010). Since the time of concentration was less than one day, it was assumed that the flow and nutrient in all the cells will reach the outlet of the watershed at the end of each time step. Thus, the model outputs at the WCW outlet (i.e., streamflow and N load) were computed as the summation of the 5,911 PRZM outputs. To represent the spatial variability of the climate, soil, and crop management, each PRZM model was individually parameterized with soil properties, land use, and management operations derived from soil databases (e.g. SSURGO), and climate and crop management scenarios. The baseline model was then set-up using the historic climate, land use, and management data to simulate the daily streamflow and N load from 2006 to 2015. Projected models were simulated for the period 2020 to 2070, and simulations were performed considering a 100-cm soil profile divided into 6 layers of 5-, 15-, and four 20-cm thickness from top to bottom.

Soil Data and land use. The soil data used in this study was collected and processed from the Soil Survey Geographic Database (USDA, 2017). A variety of soil data used in the model included bulk density (g cm⁻³), field capacity (cm³ cm⁻³), wilting point water content (cm³ cm⁻³), and organic carbon content (cm³ cm⁻³). The annual land use maps from 2005 to 2015 were collected from the USDA-NASS Cropland Data Layer (USDA, 2019). Winter wheat and pasture were the most predominant crops in WCW. All the maps came in raster format with 30 × 30 m resolution which were then processed to a 120-m pixel resolution by taking the average soil properties in the 30-m cells comprising a 120-m cell.

Managing practices and fertilizer application. For each agricultural land management practice, the planting date, harvest date, crop emergence date, and maturation date were included in the simulations to represent the growth cycle of crops. The land management data includes the time for cropping operations in the watershed such as the dates of planting, emergence, maturation, harvest, and fertilizer application. The timings for crop operations were adopted from the Agriculture Handbook No. 628 Usual Planting and Harvesting Dates for U.S. Field Crops (USDA, 1997). It should be noted however, that these dates were generated based on collected information from farmers in every state. They did not include the consideration of actual weather and field workability conditions. The fertilizer application data of the major crops in the land use map from National Land Cover Database (NLCD) (USGS, 2019) was referenced from the Oklahoma Soil Fertility

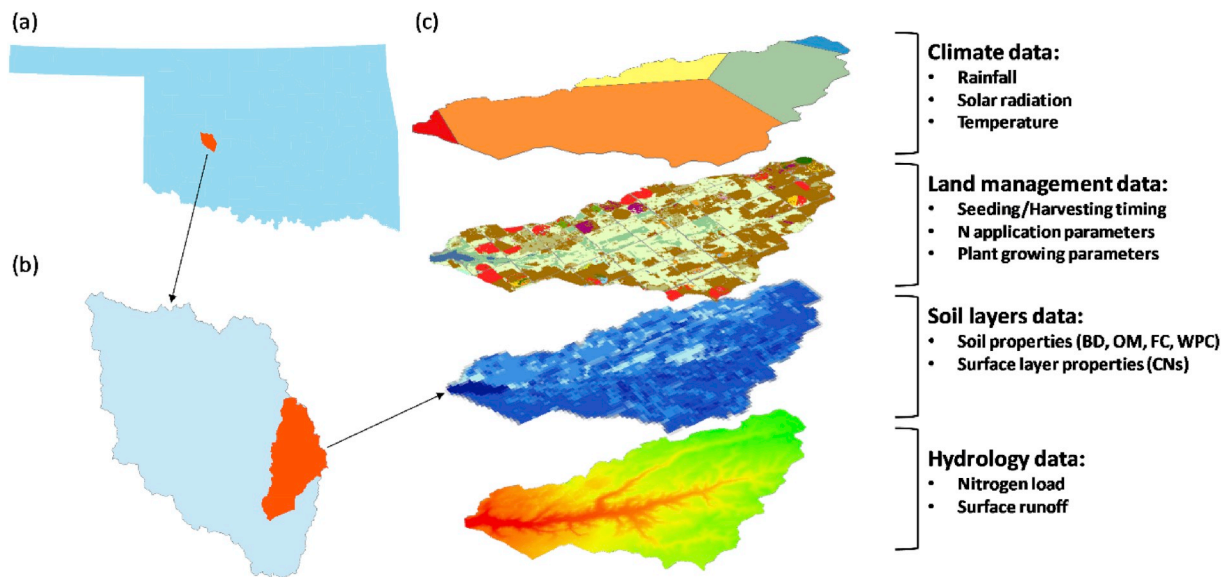


Fig. 1. (a) The FCREW in Oklahoma; (b) The WCW in FCREW; (c) Data layers used in PRZM, including climate data from five stations, land management data, soil layers data, and hydrology data.

Handbook (Zhang and Raun, 2006), National Range and Pasture Handbook (NRCS, 2003), and Oklahoma Forage and Pasture Fertility Guide (Arnall et al., 2007). The PRZM used these dates to estimate crop dynamics such as height, root depth, and canopy leaf area at each growing season. The fertilizer application inputs in PRZM requires the time, amount, and application method. To conceptualize the agricultural activities of the baseline scenario in PRZM, the following assumptions were made:

- (1) Fertilizer was applied twice a year in both spring and fall in the baseline model;
- (2) The N fixing crop decreases the amount of N fertilizer application for the other crop by 20 kg ha⁻¹ in that year for double crops in one year (NRCS, 2003; Olson and Kurtz, 1982);
- (3) For all the crops in the region, the planting day in the simulation is the middle day of the most active planting period and the harvest day in the simulation is the middle day of the most active harvest period (USDA, 1997).

Climate. The climate data used from 2006 to 2015 included daily rainfall time series, monthly average solar radiation, and monthly average temperature time series from five stations (Fig. 1c). The daily rainfall time series was obtained from the USDA- Agricultural Research Service (ARS) Micronet Network for the five stations (Fig. 1c) (Guzman et al., 2014; Starks et al., 2014). The monthly average solar fluxes were collected from the U.S. Solar Radiation Resource Map and daily maximum and minimum temperature time series were downloaded from National Centers for Environmental Information of National Oceanic and Atmospheric Administration (NOAA).

Streamflow and Nitrogen concentration. Daily streamflow and N load were needed to calibrate the historic baseline model. Daily streamflow was collected from the U.S. Geological Survey (USGS) National Water Information System database at the station of Willow Creek near Albert in Oklahoma (USGS 07325860) (Fig. 1c) from 2006 to 2015. Total N in stream (g day⁻¹) was also available from the same source at irregular intervals from 2006 to 2012 (Moriassi et al., 2014).

2.4. Model calibration

Streamflow calibration. The simulated daily surface runoff was calibrated to the observed daily surface runoff. Among the PRZM

parameters that were used in the calibration were the curve numbers, minimum depth of which evaporation is extracted, pan factor, and snowmelt factor. These parameters were adjusted to satisfy the following objective functions: (1) the cumulative simulated surface runoff matched the cumulative observed surface runoff from 2006 to 2015; and (2) the peaks in the simulated time series appeared when high surface runoff values in the observed time series were within a two-day interval. PRZM's performance in simulating the surface runoff was evaluated using the Mean Absolute Error (MAE), Percent Bias (PBIAS), Ratio of Standard Deviations (RSD), and Modified Index of Agreement (MD). The MAE and PBIAS measure the errors in the measured and simulated time series and water balance, respectively. The RSD evaluates the agreement in the distributions of the measured and simulated variables while MD is an overall "goodness of fit" indicator with 1 representing a perfect fit (Legates and McCabe, 1999).

Baseflow separation. PRZM lacks the fundamental hydrologic processes linked to the baseflow and is limited to surface runoff estimations. Therefore, it was necessary to separate the baseflow component from the measured flow to allow the comparison between measured and simulated flow and load. Baseflow separation was based on a digital filter using two-parameter Boughton algorithm; with $k = 0.99$ and $C = 0.066$ (Chapman, 1999) as follows (Eqn 1):

$$Q_b(n) = \frac{k}{1+C} Q_b(n-1) + \frac{C}{1+C} Q(n) \quad (1)$$

where:

$Q_b(n)$ is the base flow of day n (m³ s⁻¹); $Q_b(n-1)$ is the base flow of day $n-1$ (m³ s⁻¹); $Q(n)$ is the flow of day n (m³ s⁻¹); k and C are the parameters of the equation.

N load calibration. The simulated daily N load was calibrated to the sampled total N load in the stream by adjusting N application rate, application efficiency, and spray drift. It should be noted that fertilizer application is not regulated in the United States and hence, no detailed monitored data of application rates was available. The application rates, were therefore, calibrated in this study with reference to the recommended amount suggested by agricultural handbooks. Since the observed N were only available at limited intervals during the 2006–2015 period, calibrating for N was performed to satisfy the following objective functions: (1) the simulated time series was in the same magnitude as the sampled total N load; and (2) peaks in the simulated time series appeared when high sampled load values were nearby. The simulated and observed N load were compared visually.

2.5. Scenario-based changes in WCW

Scenario-based changes that included land use changes, land management practices, and climate change were implemented in WCW to determine the combination of factors that can result in critical N load (Table 1). The responses of WCW to these changes were compared with the outputs from the calibrated baseline model. Four different management factors were considered in this research including: (1) Crop rotation percentages; (2) N application rates; and (3) N application timings.

Crop rotation scenarios. The projected land use scenarios (2020–2070) were generated based on the land use maps from 2006 to 2015. Three different scenarios were considered with different percentages of two-year alfalfa crop rotation with the original crop. Alfalfa was chosen as the crop rotation plant every two years because it can improve the soil drainage situation and fix N during its growth due to its deep roots (PSA, 2017). In addition, alfalfa was regularly grown in this WCW based on the land use map from NLCD. To generate the land use practices scenarios, the land use was re-classified into three categories based on their historic land use from 2006 to 2015, and then the land management scenarios with different alfalfa crop rotation percentages were generated. Land use corresponding to open water and non-cultivated areas were left unchanged. For the baseline, the agricultural area was divided into two groups for each scenario. In the first group, a percent of cultivated area were set to allow crop rotation while the area corresponding to the second group remained unchanged. Percent of area splitting the two groups were set at 30 and 60% in a randomized approach and were changed every two years to simulate crop rotation where alfalfa would be cultivated instead of the original crop.

N application rate scenarios. The N application rate was simulated using three scenarios. In the first scenario (A0), we used the calibrated values obtained from the baseline model (Table 2). In the second scenario the recommended application rates (A1) referenced by the Oklahoma Forage and Pasture Fertility Guide were used, while in the third scenario (A2), these recommended rates were doubled (Arnall et al., 2007). When crop rotation is implemented, no fertilizer is applied to alfalfa.

N application timing scenarios. N application timing scenarios were generated based on the number of applications of N fertilizer per year. In the baseline model, N fertilizer was applied twice a year (T0), before planting and after harvesting. A one-time application scheme, during spring (TS), was adopted to determine the impacts of application timing on N load to decrease the N load during winter. In the one-time application scenario, the fertilizer application occurred in the middle of planting regardless of the projected weather conditions.

Projected climate. The climate data used from 2020 to 2070 included daily rainfall time series and daily average temperature time series while monthly average solar radiation was set to match the period from 2006 to 2015. The daily rainfall and temperature time series were obtained from the Coupled Model Intercomparison Project Phase 5 (CMIP5) multi-model dataset referenced in the Intergovernmental Panel on Climate Change Fifth Assessment Report (World Climate Research Programme, 2017). Data was downloaded from the Localized Constructed Analogs (LOCA) CMIP5 projections using the Representative Concentration Pathway 8.5 (RCP8.5) which represented the most serious global warming situation (Pierce et al., 2014). The LOCA-CMIP5 RCP8.5 ensemble is composed of 32 global circulation models from different global climate modeling groups.

Scenario combinations. Combinations of different land cover scenarios (Table 1) were simulated using the projected climate from 32 global circulation models under the LOCA ensemble. Twelve (12) land management scenarios were considered in which each model was simulated using 32 climate projections (from 2020 to 2070) for a total of 384 scenarios, each with 5,911 independent PRZM model runs. The changes in the seasonal and annual N load were evaluated across the

Table 1

Land management practices scenarios and notation used across the model simulations. CR = crop rotation (30% or 60%); T = application timing (spring or split between spring and fall); A = fertilizer application rate.

No.	Scenario	Crop Rotation (%)	Fertilizer Application	
			Timing	Rate
1	CR00T0A0	0	Spring/Fall	Baseline value
2	CR30T0A0	30	Spring/Fall	Baseline value
3	CR60T0A0	60	Spring/Fall	Baseline value
4	CR00TSA0	0	Spring	Baseline value
5	CR30TSA1	30	Spring/Fall	Recommended amount
6	CR60TSA2	60	Spring/Fall	Twice recommended amount
7	CR30TSA0	30	Spring	Baseline value
8	CR30TSA1	30	Spring	Recommended amount
9	CR30TSA2	30	Spring	Twice recommended amount
10	CR60TSA0	60	Spring	Baseline value
11	CR60TSA1	60	Spring	Recommended amount
12	CR60TSA2	60	Spring	Twice recommended amount

Table 2

Calibrated and recommended N fertilizer application rates.

Crop type	Recommended application amount (kg/ha)	Baseline application amount (kg/ha)
Corn	101	51
Cotton	68	34
Sorghum	68	34
Winter Wheat	101	51
Peanuts	336	168
Rye	68	34
Oats	101	51
Grassland/Pasture	68	34

watershed and in every cell to identify the combination of factors that can result in a critical N load. Note that the combinations of different land management schemes can result in unexpected response from the system. For instance, increasing the percentage of crop rotation can perhaps compensate for an increase in application rate. The scenarios were named according to the percentage of crop rotation (e.g., CR00, CR30, and CR60), application timing (e.g., T0 and TS), and application amount (e.g., A0, A1, A2). For instance, CR00T0A1 represents a scenario with no crop rotation, fertilizer application occurring in spring and fall, and recommended amount of N fertilizer applied.

Monthly N load analysis under different climate projections. To further analyze changes in N load under different climate projections from 2020 to 2070, monthly model outputs were used to compute the probability of occurrence of N load, and were then classified in three categories: high, moderate, and low for each land management scenario. Probability categorization were defined as: (1) High: probability corresponding to the population of N load larger than or equal to the historic monthly baseline third quartile; (2) Moderate: probability corresponding to the population of N load larger than or equal to the historic monthly baseline first quartile and less than the third quartile set to represent 50% of the N load population; (3) Low: probability corresponding of the population of N load less than the historic monthly baseline first quartile. The probability of monthly load (P_n) was computed as follows (Eqn 2):

$$P_n = \frac{M_c}{M_T} \quad (2)$$

where M_c is the number of months with N load in the category; M_T is the total number of N load in the same month per climate projection equal to 50. A ternary plot was then constructed to show the changes in the N load probability under different climate projections on monthly basis per land management scenario.

Region-based analysis. Aside from agricultural practices, the fate of

surface N also depends on the combination of factors including soil surface properties, land use, and climate. An analysis to identify cells that are “vulnerable” to high N load was performed. The cells that frequently generated the highest N load during heavy rainfall days from 2020 to 2070 were selected by the following methods:

- (1) For every climate projection, the top 1% of the total simulation period with the highest rainfall, with threshold values ranging from 25 to 33 mm/day, was selected as the days with extreme rainfall events;
- (2) Within the days with extreme rainfall events, all the cells were sorted based on their N load and the top 2.5% of the cells were selected as the most vulnerable cells under this climate projection. As 24% of the world useable land has been degraded, 2.5% is selected representing the 10% most seriously degraded soil in the degraded soil (ELD, 2014);
- (3) The frequency in which the most vulnerable cell appeared in each climate projection was computed using the baseline simulation. This frequency represents the ability of the cell to generate N via surface runoff and was referred to in this study as the Nitrogen Load Index (NLI). The cells with higher NLI tended to appear more frequently in the most vulnerable cells lists under different climate projections which suggested higher probability to generate more N load during heavy rainfall events.

To identify the factors and features that lead to higher NLI, a generalized linear model with Poisson regression was generated using the soil physical properties that are readily measurable in the field and the applied N fertilizer amount as independent variables and NLI as dependent variable. The Potential N Load Index (PNLI) of each cell in WCW was then calculated to evaluate the ability of generating N during extreme rainfall events as follows (Eqn 3):

$$PNLI = \alpha(BD) + \beta(OM) + \gamma(FC) + \delta(WPC) \quad (3)$$

where:

PNLI is the Potential Nitrogen Load Index of the region (dimensionless), BD is the bulk density of the soil surface layer (g/cm^3), OM is the organic matter mass percentage in the soil surface layer (%), FC is the volumetric field water capacity of the soil surface layer (%), WPC is the volumetric wilting point water capacity of the soil surface layer (%), and α , β , γ , and δ are the regression parameters. Cells with larger PNLI tended to generate more N load via surface runoff during days with heavy rainfall while cells with smaller PNLI tended to keep more N from being washed away by heavy rainfall.

3. Results and discussion

3.1. Model calibration

The performance of PRZM to simulate the responds of WCW was evaluated by comparing the simulated and observed streamflow and N load. The model was calibrated by changing the surface runoff and N parameters where the streamflow calibration preceded the N load calibration.

The simulated and measured cumulative flow at the end of the simulation period (2006–2016) was 188 and 189 cm, respectively (Fig. 2a). The modeling framework was able to represent the general behavior of streamflow observations with MAE of 0.06 and PBIAS of -0.60% and thus, it was assumed that it also represented the water circulation in this watershed. Note that there were no additional observations from other hydrological subsystems (e.g., groundwater, near surface) to validate the modeling framework. The RSD between the observed and simulated time series was 0.71 indicating a good match between the distributions of the two time series. Overall, the agreement between the simulated and observed surface runoff was reasonable ($MD = 0.63$).

The daily observed and simulated total N load both fell in the same order of magnitude (Fig. 2b) which was one of the objective functions that we originally aimed for. The simulated and measured peaks were also observed to occur not more than 1 day apart. Since the observed N was not a continuous time series but grab samples instead, the one-to-one comparison of the observed and simulated time series was not possible. Also, the discrepancies brought about by incorporating the baseflow, which was estimated using the Boughton algorithm, in computing the simulated total N load added another layer of uncertainty to the calibration process. The fact that PRZM only computes surface processes while measured variables include the contribution of both the surface and the baseflow (streamflow and N concentration) prevented the computation of proper metrics to quantify the model performance. Hence, the goodness-of-fit of the model was based on visual evaluation and an objective function that the simulated and observed N load should fall within the same order of magnitude.

3.2. Scenario-based simulations

Different combinations of land management scenarios were simulated to assess their corresponding impacts on N load under 32 climate projections from 2020 to 2070 (Figs. 3–5). The probabilities of high, moderate, and low N load of the different scenario combinations were plotted in a ternary plot along with the historic baseline scenario for probability analysis (Figs. 3–5).

Historic baseline in ternary plots. As the load used to determine the high and low N load were the top 25% and 75% of the historic values, respectively, the historic baseline points of all the 12 months are located at the point $(P_{\text{high}}, P_{\text{mid}}, P_{\text{low}}) = (0.25, 0.5, 0.25)$ in the ternary plot. The unchanged location of the historic baseline points, indicated by a black square (e.g. Fig. 3), provided a visual analysis of expected changes in the occurrence of N load compared to the baseline under future scenarios. In the plot, the land management scenarios with more points in the upper vertex were expected to generate less high N load events compared to those in the lower left vertex. Therefore, the upper tip of the ternary graph, where $P_{\text{high}} = 0$ and $P_{\text{low}} = 1$, is the most sought-after condition. The plots can also be used to analyze the monthly N load behavior between different months.

3.3. Effects of projected climate

The projected annual mean rainfall from 2020 to 2070 is expected to increase on average by approximately 17% compared to the baseline rainfall from 2006 to 2015. Yet, the annual mean N load of scenario CR00T0A0, which was the projection of the historic baseline from 2020 to 2070, remained the same as the historic baseline from 2006 to 2015. Furthermore, the peak monthly N load was observed to occur one month earlier in the projected scenario compared to the baseline which can be due to the shift in the rainfall peak from June in the historic to May in the projected climate. However, the maximum monthly N load increased by approximately 43% compared to the historic baseline mean and this percentage rose to 1000% in January, which suggested that the monthly N load can reach a very high level under some climate projections.

The probability analysis showed that significant changes in monthly N load probability distribution may take place from 2020 to 2070 (Fig. 3a). The ternary plot for the projected baseline scenario, CR00T0A0 (Fig. 3a) showed that high monthly load from March to May and from November to February were expected to happen more frequently compared to the historic baseline ($P_{\text{high}} > 0.25$). In fact, the occurrence of high N load was expected to be more than 75% for these months from 2020 to 2070. Meanwhile, the frequency of high monthly N load from June to October were expected to decrease from 2020 to 2070. The possible reasons for these changes in the probability distribution of the monthly load from 2020 to 2070 included: (1) The peak rainfall shift from June to May in the future climate projections was

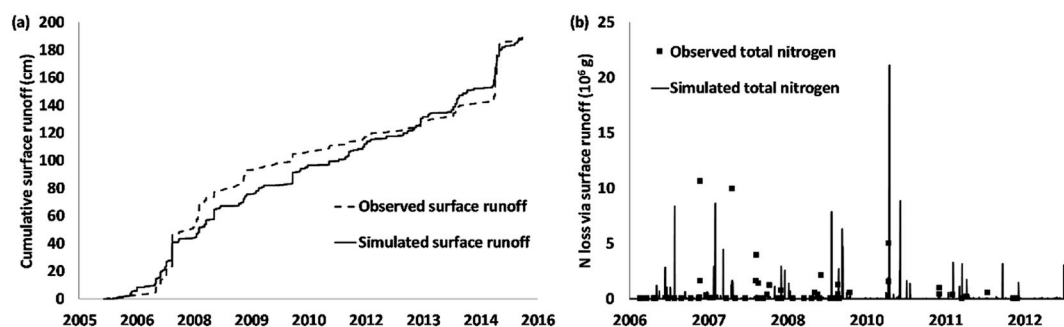


Fig. 2. (a) Daily simulated and observed cumulative surface runoff; (b) Comparison between simulated N load and measured N from grab samples (i.e., instantaneous measurements of N taken at specific times).

expected to generate more surface runoff in May; (2) Climate changes resulted in generating more and heavier rainfall events which increased the frequency of high N load months in the future; and (3) The plants were expected to have more canopy past June resulting in more interception and less surface runoff.

3.4. Land management scenarios

Among the 12 land management scenarios simulated in this research, four of them were intended to reduce N load. These were 30% and 60% crop rotation combined with single fertilizer application or double fertilizer applications (Fig. 4b–e). Another four scenarios (Fig. 5b–e) were intended to analyze the tradeoffs between higher economic benefits and environmental welfare. These scenarios combined 30% and 60% crop rotation with increased application rates to determine if the effects of crop rotation can offset the impacts of increased N concentration from fertilizer.

Single application: The impacts of the application timing were evaluated using scenarios CR00T0A0 and CR00TSA0 through the monthly mean N load and the probability distribution among high, moderate, and low-level N load. Based on the results, the annual N load increased by 4% when the land management practice changed from

spring-fall application (T0) to spring application (TS). Specifically, the monthly N load increased in May, June, July, and August (Fig. 3c) in response to a full fertilizer application rate as opposed to a split load in spring-fall application. However, the probability analysis showed that the occurrence of high N load events (P_{high}) has decreased apart from May, June, and July, although P_{high} for June and July is still below the historic baseline. Results suggested that spring application was capable of decreasing N load in most of the year at the cost of larger probability of high N load occurrences from May to July. However, research also showed that spring-fall application practice was expected to be more efficient since smaller amounts are timed to match major crop uptake periods (Edwards et al., 2006; Sowers et al., 1994).

Crop rotation in split application: The impacts of crop rotation were evaluated using scenarios with different percentages of crop rotation cover (alfalfa) combined with spring-fall fertilizer application (T0). Scenarios CR30T0A0 and CR60T0A0 are examples of crop rotation variation in the watershed with fertilizer application in spring and fall. Overall, increasing the area where crop rotation was implemented in the watershed decreased N load since less N was applied on the soil compared with the scenario CR00T0A0 during the simulation period (Fig. 4f). However, no notable differences were observed in the probability of occurrence of high N load (P_{high}) with these scenarios (Fig. 4b

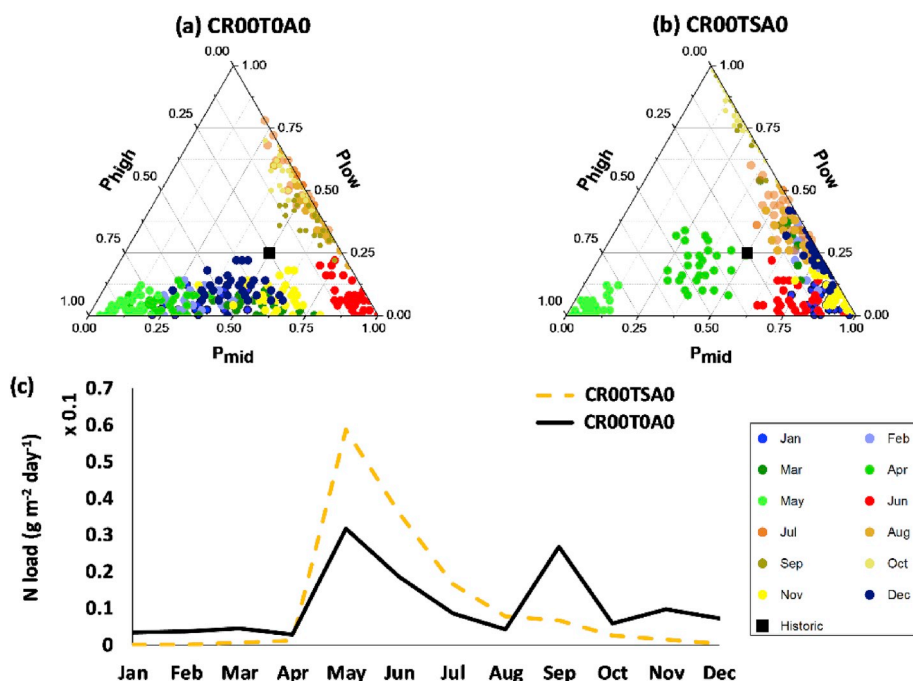


Fig. 3. Monthly N load probability distribution ternary plots of the scenarios with (a) spring-fall applications and (b) spring applications, and (c) monthly mean N load from 2020 to 2070.

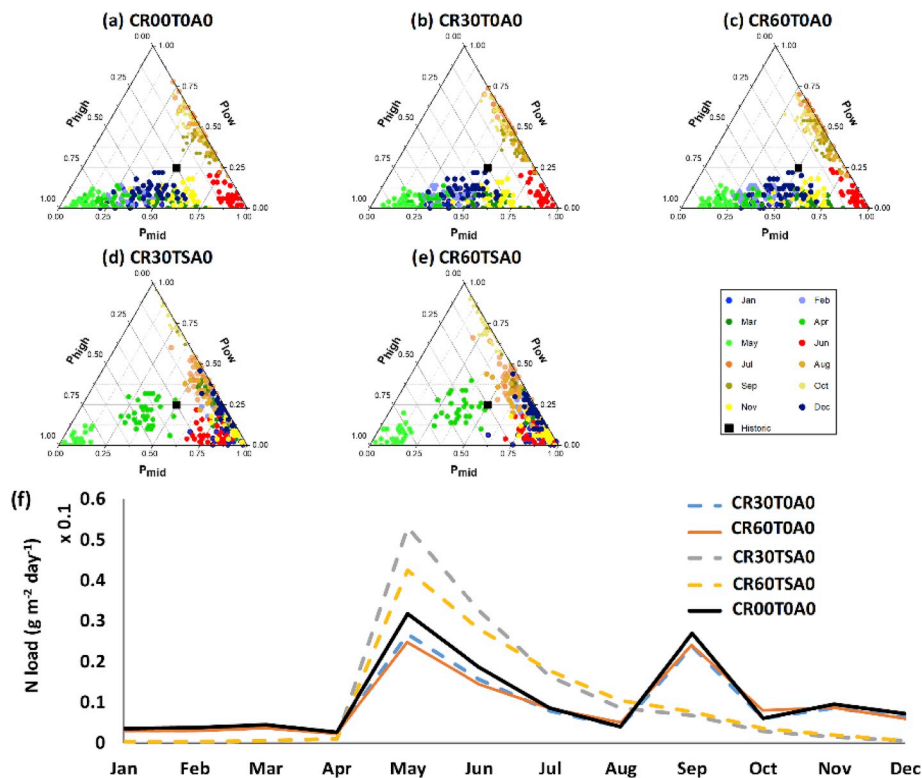


Fig. 4. Monthly N load probability distribution ternary plots of the scenarios with different areas of crop rotation and (a, b, and c) spring and (d and e) spring-fall application under the baseline fertilizer application rate, and (f) their monthly mean N load from 2020 to 2070.

and c) compared with the CR00T0A0 scenario (Fig. 4a) for months with high P_{high} ($P_{high} > 75\%$). Additionally, unexpected increase in the monthly mean N load in August and October was observed in these scenarios compared with the CR00T0A0 from 2020 to 2070. This increase in N load in surface runoff was associated with the low canopy interception depth of alfalfa which was usually harvested every 35–49 days leaving the soil with less cover. Smaller canopy interception of rainfall was expected to generate higher surface runoff because PRZM simulated precipitation reaching the soil surface by subtracting plant interception first from the total precipitation. Smaller interception would result in more precipitation available for surface runoff. As curve number remained the same in the simulation, more precipitation reaching the soil surface would result in more surface runoff. In summary, increasing the coverage of crop rotation practice was expected to lower the N load but at the cost of increasing the occurrence of high N load events (P_{high}) in August and October.

Crop rotation and single application: The combined impacts of crop rotation and single application land management practice were evaluated using different percentages of crop rotation cover with annual spring application. Scenarios CR30TSA0 and CR60TSA0 are examples of crop rotation variation under single application in the watershed. Overall, the annual mean N load remained the same as that in CR00T0A0 during the simulation period. However, a significant increase in April and May N load was observed while the rest of the months posed decreases in N load (Fig. 4f). This increase in April and May was because the N fertilizer application in spring doubled resulting in high N concentration in the soil surface in the months of April and May. After two months of plants absorption, leaching, and surface runoff, the N concentration in the soil surface was expected to drop which decreased the N load from surface runoff in the rest of the year. However, the probability analysis showed greater potential of single application in reducing the occurrence of high N load events ($P_{high} < 0.75$). In fact, only four climate projections in June and 2 projections in January were expected to generate high N load more

frequently than historic baseline by implementing 30% area of crop rotation (Fig. 4d and e). If 60% of the area is converted to crop rotation, P_{high} of all the months besides April and May reduced to around 10% which meant that the probabilities of high N monthly load dropped to half of the baseline (Fig. 4d and e). These results suggested that the N high monthly load appeared much less frequently from June to March by applying both single application and crop rotation practice.

Increase in application rates. The monthly N load in surface runoff of scenarios CR30T0A1 and CR60T0A2 were compared with the scenario CR00T0A0 to determine if larger crop rotation area could reduce the N load even when the application rate was increased. The calibrated application rates (A0) for different crops in the baseline model are shown in Fig. 2 together with the rates recommended (A1) by the Oklahoma Forage and Pasture Fertility Guide (Arnall et al., 2007). Scenario CR30T0A1 combined the effects of 30% crop rotation and the recommended amount of fertilizer while CR60T0A2 determines the tradeoffs between increasing the fertilizer amount to twice the recommended and implementing higher crop rotation coverage. In both scenarios, the fertilizer was applied in fall and spring. Based on the results, a notable increase in the mean N load was observed in scenarios CR60T0A2 and CR30T0A1 compared with the baseline scenario. Furthermore, comparison of the monthly peak values indicated that the expected monthly peak load could increase to up to 680% of baseline in CR60T0A2 and 320% in CR30T0A1 (Fig. 5f). Also, the frequency of occurrence of high N load events increased when the application rate increased regardless of the increase in crop rotation coverage. Comparison between the ternary plots of these scenarios and CR00T0A0 (Fig. 5a–c) showed that the dots started moving towards the left vertex of the triangle when the application rate was increased.

The impacts of spring application, increased application rate, and crop rotation were determined in scenarios CR30TSA1 and CR60TSA2 (Fig. 5d and e). Overall, the crop rotation and spring application were not expected to offset the negative environmental effects from the doubled N fertilizer application rate. The increase in N load was more

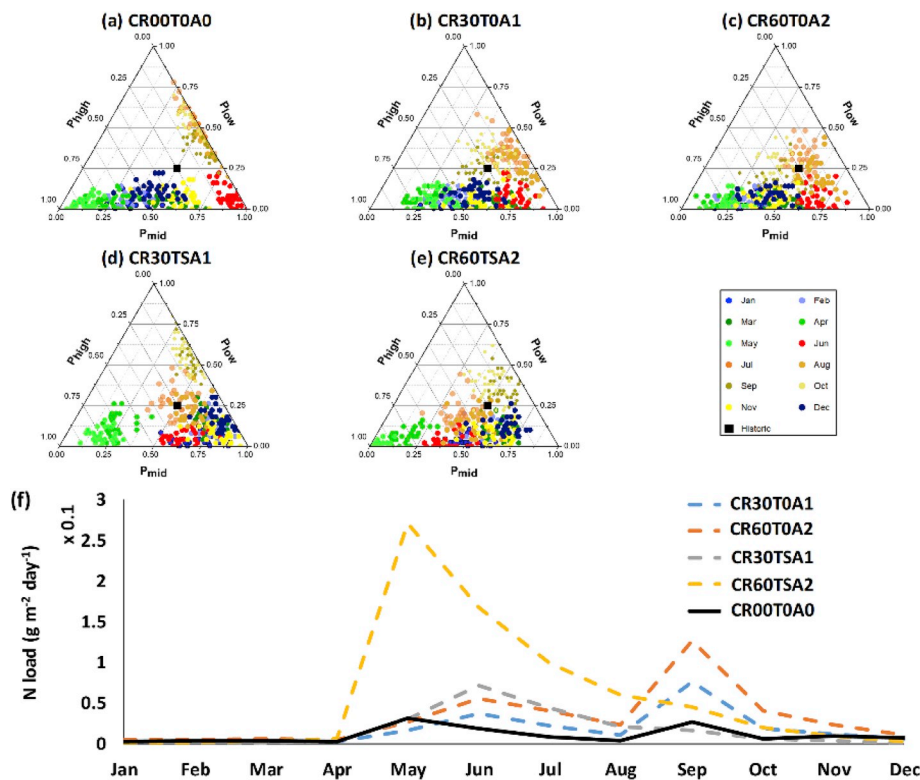


Fig. 5. Monthly N load probability distribution ternary plots of the scenarios combining different areas of crop rotation with (a, b, and c) spring-fall or (d and e) spring application under the recommended or double the recommended amount of N fertilizer applied, and (f) their monthly mean N load from 2020 to 2070.

than 800% from May to August which meant that the average N load level was expected to be kept at high level during summer (Fig. 5f). However, crop rotation combined with spring application was expected to keep the N load the same as the historic baseline when the recommended rate of N fertilizer was applied during most of the year. Based on Fig. 4d, the occurrence of high monthly N load was kept at the same level as historic in all the months except April and May. In summary, our results revealed that increasing crop rotation area combined with spring application was expected to cancel the negative effects of N fertilizer at recommended application rate. However, neither crop rotation nor spring-application was expected to lower the N load to the historic level.

3.5. Region-based analysis

The Nitrogen Load Index (NLI) of every agricultural region was generated to determine the general behavior of the region in generating N load during a storm event. Based on the generalized linear model with Poisson distribution, we found that a soil surface with higher bulk density, organic matter, and field water capacity was expected to lose less N load during heavy rainfall events. On the other hand, a soil surface with higher wilting point water capacity and higher application N rate was expected to generate more N load during heavy rainfall events.

To eliminate the effects of different N application rates on NLI, the PNLI of every agricultural region in WCW watershed was calculated to evaluate the ability of losing N during extreme rainfall events based on the regression model of NLI. After fitting a Poisson distribution to the data, the regression parameters α , β , γ , and δ were found to be -47 , -0.464 , -3.37 , and 4.18 , respectively, with $p < 0.01$. The resulting equation for PNLI was as follow (Eqn 4):

$$PNLI = -47*BD - 0.464*OM - 3.37*FC + 4.18*WPC \quad (4)$$

3.6. Customized land management

The N load from the watershed during days with heavy rainfall was expected to decrease if we re-assign the land uses based on their PNLI (Fig. 6b). To reduce the N load without applying less N in the field, the agricultural cells in baseline land use from 2020 to 2070 were assigned new land use scenarios to specifically target what the cells require to lower the N load. Since the application rate was found to be the dominant factor that controls the N load, the land use scenarios with higher mean annual N fertilizer application rate were assigned to the cells with lower PNLI. The new scenario was then simulated under 32 climates from 2020 to 2070 to determine the effects of the redistribution of land use.

By applying the N fertilizer based on the PNLI of the soil cells, the monthly N maximum value decreased by 13.4% and the annually mean N load decreased by 6.1% (Fig. 6b). In addition, the most critical month also changed from September to May. As discussed above, lower and earlier N load peaks were expected to cause less environmental problems to the watershed ecosystems due to the lower water temperature. In addition, the occurrence of months with high N load and moderate N load also decreased from May to October which indicated that the target application management was expected to improve the N load behavior (Fig. 6a). However, as only the N load in surface runoff was considered in changing land management practices, the effects of target application management on the economic benefits were unclear. It was assumed that increasing the application rate can increase the productivity of the system.

Customized field scale land management practices can be implemented following the methodology illustrated in this study. Identifying areas that are most vulnerable to surface runoff and N loss and targeting specific practices to mitigate this can result in a more sustainable farming system where productivity and environmental soundness are optimized. Due to the spatial variability of factors affecting transport processes, this approach is expected to result in a more

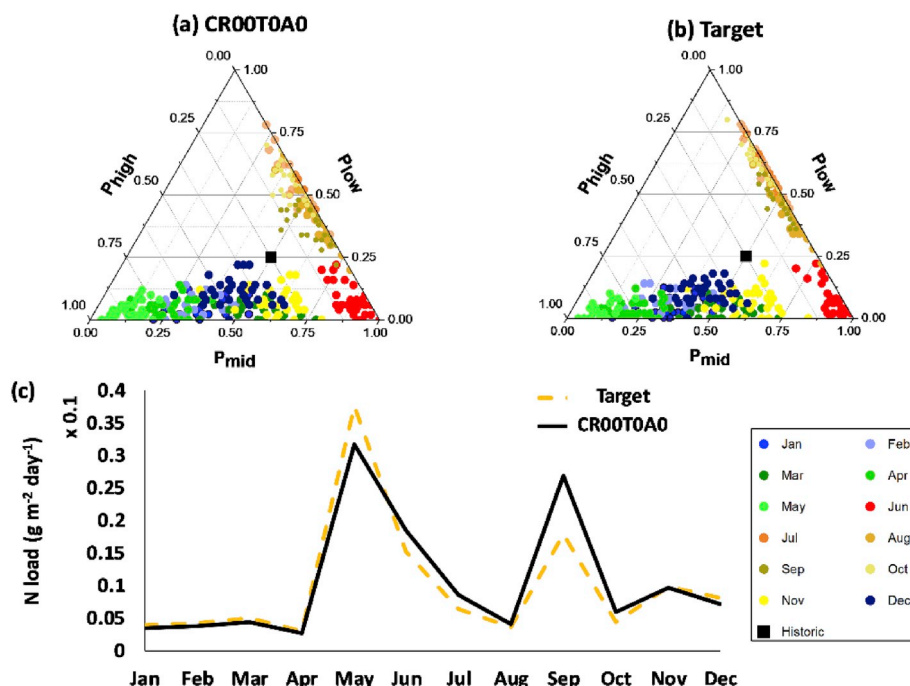


Fig. 6. Monthly N load probability distribution ternary plots of (a) the projected baseline and (b) the target application management scenarios, and (c) monthly mean N load from 2020 to 2070.

efficient use of resources than when land management is implemented across an entire area.

4. Conclusions

This study evaluated the effects of different land management practices on N load in surface runoff under future climate projections at the field scale level. The combinations of land management practices were also evaluated to determine those that can increase productivity with minimal negative impacts on the environment. Moreover, this study developed a methodology to identify areas most vulnerable to generate N load in surface runoff and to target specific management to these areas. Based on our results, crop rotation practices lowered both the N load and the probability of high N load. Furthermore, when fertilizer is applied during spring instead of the split spring-fall application, crop rotation can cancel the negative effects of increasing the fertilizer rate to the recommended amount. Spring application reduced the negative effects in summer and fall from other land managements but at the risk of increased probability of generating high N load in April and May. Our results also confirmed that fertilizer application rate was the most critical factor in determining both the amount and the probability of high N load. To address this issue, the target application management approach could be implemented at the field scale to customize land management practices to reduce the amount and probability of high N load.

Acknowledgement

Funding for this research was provided by the U.S. Department of Agriculture – National Institute for Food and Agriculture (NIFA) project [# ILLU-741-380].

Appendix A. Supplementary data

Supplementary data to this article can be found online at <https://doi.org/10.1016/j.jenvman.2019.109327>.

References

- Arnall, B., Redfearn, D., Hanks, T., Jones, J., Payne, J., Penn, C., Pugh, B., Rice, C., Warren, J., Zhang, H., Eller, T., Hiner, G., 2007. Oklahoma Forage and Pasture Fertility Guide. Stillwater.
- Chapman, T., 1999. A comparison of algorithms for streamflow recession and baseflow separation. *Hydrol. Process.* 13, 701–714. 2-2. [https://doi.org/10.1002/\(SICI\)1099-1085\(19990415\)13:5%3C;701::AID-HYP774%3E;3.0.CO](https://doi.org/10.1002/(SICI)1099-1085(19990415)13:5%3C;701::AID-HYP774%3E;3.0.CO).
- Chen, L., Messing, I., Zhang, S., Fu, B., Ledin, S., 2003. Land use evaluation and scenario analysis towards sustainable planning on the Loess Plateau in China - case study in a small catchment. *Catena* 54, 303–316. [https://doi.org/10.1016/S0341-8162\(03\)00071-7](https://doi.org/10.1016/S0341-8162(03)00071-7).
- Douglas Jr., C.L., King, K.A., Zuzel, J.F., 1998. Nitrogen and phosphorus in surface runoff and sediment from a wheat-pea rotation in Northeast Oregon. *J. Environ. Qual.* 27, 1170–1177.
- Edwards, J., Godsey, C., Raun, B., Taylor, R., 2006. Fall Nitrogen Requirements for Winter Wheat 18.
- ELD, T.E. of L.D., 2014. A Global Initiative for Sustainable Land Management.
- Guzman, J.A., Chu, M.L., Starks, P.J., Moriasi, D.N., Steiner, J.L., Fiebrich, C.A., McCombs, A.G., 2014. Upper washita river experimental watersheds: data screening procedure for data quality assurance. *J. Environ. Qual.* 43, 1250. <https://doi.org/10.1515/bchm2.1927.163.4-6.229>.
- Jamieson, R.C., Gordon, R.J., Tattler, S.C., Stratton, G.W., 2003. Sources and persistence of fecal coliform bacteria in a rural watershed. *Water Qual. Res. J.* 38, 33–47. <https://doi.org/10.2166/wqrj.2003.004>.
- Legates, D.R., McCabe, G.J., 1999. Evaluating the use of “goodness-of-fit” measures in hydrologic and hydroclimatic model validation. *Water Resour. Res.* 35, 233–241. <https://doi.org/10.1029/1998WR900018>.
- Moriasi, D.N., Guzman, J.A., Steiner, J.L., Starks, P.J., Garbrecht, J.D., 2014. Seasonal sediment and nutrient transport patterns. *J. Environ. Qual.* 43, 1334. <https://doi.org/10.2134/jeq2013.11.0478>.
- Nendel, C., Berg, M., Kersebaum, K.C., Mirschel, W., Specka, X., Wegehenkel, M., Wenkel, K.O., Wieland, R., 2011. The MONICA model: testing predictability for crop growth, soil moisture and nitrogen dynamics. *Ecol. Model.* 222, 1614–1625. <https://doi.org/10.1016/j.ecolmodel.2011.02.018>.
- NRCS, 2017. Land use - about the data | NRCS. [WWW Document]. URL. <https://www.nrcs.usda.gov/wps/portal/nrcs/detail/national/technical/?cid=stelprdb1083122> (accessed 12.12.17).
- NRCS, 2003. National Range and Pasture Handbook.
- Olson, R.A., Kurtz, L.T., 1982. Crop nitrogen requirements, utilization, and fertilization. In: *Nitrogen in Agricultural Systems*, pp. 437–504. <https://doi.org/10.2134/agronmonogr49.c12>.
- Pierce, D.W., Cayan, D.R., Thrasher, B.L., 2014. Statistical downscaling using localized constructed Analogs (LOCA)*. *J. Hydrometeorol.* 15, 2558–2585. <https://doi.org/10.1175/JHM-D-14-0082.1>.
- PSA, P.S.A., 2017. 2014 commodity fact sheet 5625, 70–75. <https://doi.org/10.1023/2FA-3A101117412693>.
- Schilling, K.E., Wolter, C.F., 2009. Modeling nitrate-nitrogen load reduction strategies for

- the des moines river, Iowa using SWAT. *Environ. Manag.* 44, 671–682. <https://doi.org/10.1007/s00267-009-9364-y>.
- Sowers, E., Pan, L., Miller, B.C., Smith, J.L., 1994. Nitrogen Use Efficiency of Split Nitrogen Applications in Soft White Winter Wheat (AJ) 942–948. (1994).
- Starks, P.J., Fiebrich, C.A., Grimsley, D.L., Garbrecht, J.D., Steiner, J.L., Guzman, J.A., Moriassi, D.N., 2014. Upper washita river experimental watersheds: meteorologic and soil climate measurement networks. *J. Environ. Qual.* 43, 1239. <https://doi.org/10.2134/jeq2013.08.0312>.
- Suárez, L.A., 2005. PRZM-3. A Model for Predicting Pesticide and Nitrogen Fate in the Crop Root and Unsaturated Soil Zones: Users Manual for Release, vol. 3 12.2.
- Timmons, D.R., Burwell, R.E., Holt, R.F., 1973. Nitrogen and phosphorus losses in surface runoff from agricultural land as influenced by placement of broadcast fertilizer. *Water Resour. Res.* 9, 658–667. <https://doi.org/10.1029/WR009i003p00658>.
- Tuppad, P., Santhi, C., Wang, X., Williams, J.R., Srinivasan, R., Gowda, P.H., 2010. Simulation of conservation practices using the apex model. *Appl. Eng. Agric.* 26, 779–794. <https://doi.org/10.13031/2013.34947>.
- Turner, N.C., 2004. Agronomic options for improving rainfall-use efficiency of crops in dryland farming systems. *J. Exp. Bot.* 55, 2413–2425. <https://doi.org/10.1093/jxb/erh154>.
- University of Oklahoma, 2017. Oklahoma Climatological Survey.
- USDA, 2019. USDA - national agricultural Statistics Service homepage. [WWW Document]. URL. <https://www.nass.usda.gov/> (accessed 7.21.19).
- USDA, 2017. Description of SSURGO database | NRCS soils. [WWW Document]. URL. https://www.nrcs.usda.gov/wps/portal/nrcs/detail/soils/survey/geo/?cid=nrcs142p2_053627 (accessed 12.12.17).
- USDA, 2010. National Engineering Handbook Chapter 15 Time of Concentration. USDA, 1997. Usual Planting and Harvesting Dates for U.S. Field Crops.
- USGS, 2019. National land cover database. [WWW Document]. URL. https://www.usgs.gov/centers/eros/science/national-land-cover-database?qt-science_center_objects=0#qt-science_center_objects (accessed 7.21.19).
- Wang, Y., Bian, J., Zhao, Y., Tang, J., Jia, Z., 2018. Assessment of future climate change impacts on nonpoint source pollution in snowmelt period for a cold area using SWAT. *Sci. Rep.* 8, 1–13. <https://doi.org/10.1038/s41598-018-20818-y>.
- Williams, J.R., 1975. SEDIMENT ROUTING FOR AGRICULTURAL WATERSHEDS. *J. Am. Water Resour. Assoc.* 11, 965–974. <https://doi.org/10.1111/j.1752-1688.1975.tb01817.x>.
- Williams, J.R., Izaurralde, R.C., Williams, C., Steglich, E.M., 2015. Agricultural Policy/Environmental eXtender Model Theoretical Documentation Version 0806.
- World Climate Research Programme, 2017. CMIP5 - overview. [WWW Document]. URL. <https://cmip.llnl.gov/cmip5/index.html?submenuheader=0> (accessed 12.12.17).
- Zhang, H., Raun, W.R., 2006. Oklahoma Soil Fertility Handbook 2006 140.